



HAL
open science

MONITORING COMPOSITION AND STRUCTURE OF MOCVD ZrO₂-BASED MULTICOMPONENT FILMS BY INNOVATIVE MIXED METAL-ORGANIC PRECURSORS

Vladislav V. Krisyuk, Diane Samélor, Asiya E. Turgambaeva, Jérôme Esvan,
Ilya V. Korolkov, Evgeny A. Maksimovskiy, Sergey V. Trubin, Yu V.
Shevtsov, Constantin Vahlas

► **To cite this version:**

Vladislav V. Krisyuk, Diane Samélor, Asiya E. Turgambaeva, Jérôme Esvan, Ilya V. Korolkov, et al.. MONITORING COMPOSITION AND STRUCTURE OF MOCVD ZrO₂-BASED MULTICOMPONENT FILMS BY INNOVATIVE MIXED METAL-ORGANIC PRECURSORS. *Journal of Structural Chemistry*, 2020, 61 (11), pp.1729-1739. 10.1134/S0022476620110074 . hal-03177409

HAL Id: hal-03177409

<https://hal.science/hal-03177409>

Submitted on 23 Mar 2021

HAL is a multi-disciplinary open access archive for the deposit and dissemination of scientific research documents, whether they are published or not. The documents may come from teaching and research institutions in France or abroad, or from public or private research centers.

L'archive ouverte pluridisciplinaire **HAL**, est destinée au dépôt et à la diffusion de documents scientifiques de niveau recherche, publiés ou non, émanant des établissements d'enseignement et de recherche français ou étrangers, des laboratoires publics ou privés.






Open Archive Toulouse Archive Ouverte (OATAO)

OATAO is an open access repository that collects the work of Toulouse researchers and makes it freely available over the web where possible

This is an author's version published in: <http://oatao.univ-toulouse.fr/27487>

Official URL: <https://doi.org/10.1134/S0022476620110074>

To cite this version:

Krisyuk, Vladislav V. and Samélor, Diane  and Turgambaeva, Asiya E. and Esvan, Jérôme  and Korolkov, Ilya V. and Maksimovskiy, Evgeny A. and Trubin, Sergey V. and Shevtsov, Yu V. and Vahlas, Constantin 
MONITORING COMPOSITION AND STRUCTURE OF MOCVD ZrO₂-BASED MULTICOMPONENT FILMS BY INNOVATIVE MIXED METAL-ORGANIC PRECURSORS. (2020) *Journal of Structural Chemistry*, 61 (11). 1729-1739. ISSN 0022-4766

Any correspondence concerning this service should be sent to the repository administrator: tech-oatao@listes-diff.inp-toulouse.fr

MONITORING COMPOSITION AND STRUCTURE OF MOCVD ZrO₂-BASED MULTICOMPONENT FILMS BY INNOVATIVE MIXED METAL-ORGANIC PRECURSORS

V. V. Krisyuk^{1*}, D. Samélor²,
A. E. Turgambaeva¹, J. Esvan², I. V. Korolkov¹,
E. A. Maksimovskiy¹, S. V. Trubin¹,
Yu. V. Shevtsov¹, and C. Vahlas²

Three volatile mixed-metal precursors [ZrL₄Pb(hfa)₂] (**1**), [ZrL₄PbL₂] (**2**), and [ZrL₄La(dpm)₃] (**3**) (L = 2-methoxy-2,6,6-trimethyl-3,5-heptanedionate; dpm = 2,2,6,6-tetramethyl-3,5-heptanedionate; hfa = 1,1,1,5,5,5-hexafluoro-2,4-pentanedionate) are used to prepare ZrO₂-based multicomponent films by metalorganic chemical vapor deposition (MOCVD). The deposition experiments are carried out in a hot-wall reactor at 600-750 °C on silicon substrates under 20 Torr in the presence of oxygen. According to X-ray powder diffraction, the main crystal phases in the films prepared from precursors **1** and **2** are solid solutions based on tetragonal and cubic ZrO₂. Lead does not form separate crystal phases but is dissolved in the oxide form within the ZrO₂ matrix, as is indicated by X-ray photoelectron spectroscopy data. La₂Zr₂O₇ films are prepared from **3** using two ways of precursor supply: evaporation in argon and by direct liquid injection (DLI). It is shown that the composition and structure of obtained films are determined by the precursor composition. The results obtained for thermal behavior of precursors in condensed and gas phases are discussed.

DOI: 10.1134/S0022476620110074

Keywords: metal β-diketonates, thermal properties, mixed metalorganic precursors, zirconia based films, multicomponent films, MOCVD.

INTRODUCTION

Films based on zirconium dioxide ZrO₂ are widely used in the production of various functional materials and coatings. In particular, rare earth zirconates (Ln₂Zr₂O₇) exhibit high melting-point values, exceptional ionic conductivity, high radiation and chemical resistances, and low thermal conductivity, so they are interesting materials for the preparation of thermal barrier coatings (TBCs) for gas turbines [1], solid oxide fuel cells (SOFCs) [2], in radioactive waste processing [3], and fabrication of gas sensors and catalysts [4]. Thin ferroelectric lead-zirconate-titanate films (PbZr_{1-x}Ti_xO₃ or PZT) can be used in semiconductor devices to prepare nonvolatile random-access memories (NVRAMs) with long endurance and high-speed access [5].

Metalorganic chemical vapor deposition (MOCVD) is virtually beyond the competition as far as the production of films with complex surface geometries [6]. However, multicomponent inorganic films meet also some technical

¹Nikolaev Institute of Inorganic Chemistry, Siberian Branch, Russian Academy of Sciences, Novosibirsk, Russia; *kvv@niic.nsc.ru. ²Interuniversity Materials Research and Engineering Centre (CIRIMAT), CNRS, Toulouse, France.

complications (using multiple precursor vapor sources) as well as complications of achieving exact stoichiometry of metal-containing phases. Such films can be prepared from a single vapor source by metalorganic chemical vapor deposition using mixed-metal precursors (either individual heterometallic complexes or mixtures of metal–dopant complexes and zirconium) [7, 8]. The design of novel heterometallic compounds to be used for the deposition of multicomponent inorganic films and coatings requires proper organic ligands. The latter should bind at least two different metals within one molecule and preserve the volatility of resulting compounds, since this property is critical for the precursor to be used in MOCVD. The problem of preparing films with required component ratios can be partially solved by using heterometallic precursors. We earlier demonstrated the possibility of using copper-palladium precursors based on methoxy-substituted diketonate ligands (containing a methoxy group in the terminal substitute) to prepare bimetallic alloy films [9, 10]. It was shown that precursors with the same 1:1 metal ratio and different ligands result (other conditions being equal) in Cu–Pd films of different composition. In one case, the ratio of metals in the films depended on the deposition temperature, since the complex dissociated into monometal fragments as a result of thermolysis on the heated substrate. In another case, the ratio of metals in the films was ~1:1 due to the fact that the initial complex was resistant to dissociation. Thus, the metal ratio of the heterometallic compound is not always preserved, since the components can be partially removed in the form of volatile products as a result of the heterocomplex thermolysis on the substrate, i.e. the result depends on the balance of chemical bond energies in the precursor molecule. Mixtures of monometallic complexes are not always appropriate due to the requirement of similar thermal properties [7]: in particular, it is difficult to obtain an inorganic film with a specified ratio of metals by mixing components with very different volatilities. To obtain the required ratio of phases or components in the resulting material, one has to study how thermal properties of heterometallic precursors depend on their composition and structure. Note that the MOCVD of mixed oxide films employed mainly precursors containing alkoxide ligands such as $\text{BaSn}_2(\text{O}t\text{-Bu})_6$ [8], $\text{Et}_3\text{Pb}(\text{O}t\text{-Bu})\text{Zr}(\text{O}t\text{-Bu})_4$, and $\text{Et}_3\text{Pb}(\text{O}t\text{-Bu})\text{Ti}(\text{O}t\text{-Bu})_4$ [11]. Heterometallic complexes based on β -diketonates and their derivatives were also used to prepare mixed-metal oxides [12, 13].

The present work reports preliminary results obtained for the properties and structure of multicomponent ZrO_2 -based films prepared from mixed Zr-containing precursors. In order to optimize the deposition process, including the composition and the ratio of desired metal-containing phases in the film, one has to understand how the properties of the precursor depend on its composition and structure. Therefore, we studied the composition and structure of multicomponent films prepared by chemical deposition of precursor vapors. The precursors were obtained by co-crystallization of zirconium complexes with lead and lanthanum complexes. β -Diketones, including methoxy-substituted ones, were used as ligands (Fig. 1). The thermal properties of new precursors were compared using comprehensive thermal analysis. An original mass spectrometric technique was used to study the gas phase composition upon heating the precursors and to estimate the thermal stability and composition of gaseous thermolysis products of precursor vapors. The resulting compounds were tested as MOCVD precursors in a hot-wall reactor. For the La–Zr system, the films prepared by direct liquid injection (DLI MOCVD) were also studied.

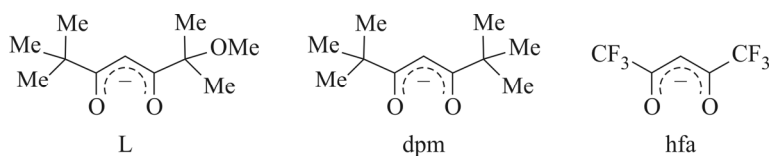


Fig. 1. Structural formulas of chosen β -diketonate ligands: L = 2-methoxy-2,6,6-trimethyl-3,5-heptanedione; dpm = dipivaloylmethanate: 2,2,6,6-tetramethyl-3,5-heptanedione; hfa = hexafluoroacetylacetonate: 1,1,1,5,5,5-hexafluoro-2,4-pentanedionate.

EXPERIMENTAL

Preparation of precursors

The synthesis of mixed-metal precursors was performed using freshly sublimated homometallic complexes. The preparation of initial complexes $\text{Pb}(\text{hfa})_2$, PbL_2 , ZrL_4 , and $\text{La}(\text{dpm})_3$ was described in [14-16]. The batches were mixed in pairs of ZrL_4 with $\text{Pb}(\text{hfa})_2$ (PbL_2 , $\text{La}(\text{dpm})_3$) in equimolar combinations per 300 mg ZrL_4 and dissolved in a 1:1 mixture of equal volumes of toluene+heptane solvents in graduated cells for crystal growth. The prepared solutions were placed in special chambers where the solvent was slowly evaporated in a dry nitrogen flow. As a result of complete evaporation, white crystalline samples $[\text{ZrL}_4\text{Pb}(\text{hfa})_2]$ (**1**), $[\text{ZrL}_4\text{PbL}_2]$ (**2**), $[\text{ZrL}_4\text{La}(\text{dpm})_3]$ (**3**) were obtained. Precursors **1-3** were dried in a vacuum desiccator over CaCl_2 to constant weight. The weight of final samples did not exceed the total weight of the batches of initial complexes. The obtained precursors **1-3** without additional purification were used to study thermal properties and the deposition of films.

Thermal analysis (TG-DTA) of precursors

The TG-DTA was carried out using a TG 209 F1 Iris (NETZSCH) thermal balance. The decomposition of compounds was performed in helium (30 mL/min) in a temperature region of 25-500 °C and a heating rate of 10 °C/min. The ~10 mg samples were placed in open quartz crucibles.

Mass spectrometric study

The study was carried out on a "MSKh"-6 time-of-flight mass spectrometer equipped with a special system of sample vapor injection into the ion source. The system is a built-in miniature low-pressure hot-wall CVD reactor equipped with an independently heated evaporator [17]. The ionization was achieved by electrons, the ionization energy was 70 eV. The studied compound (~1 mg) in an open glass cell was placed in the evaporator which was heated to T_{ev} (see the Table 1) after evacuation. This temperature remained constant throughout the experiment. The vapor of the studied sample was supplied into the reactor and then passed through the effusion hole into the ion source. When measuring the thermal stability of vapors, the reactor was heated linearly with a rate of 5 deg/min.

MOCVD experiments

The experiments were carried out in a hot-wall quartz reactor (shown schematically in Fig. 2) using an injection system of precursor free evaporation in the carrier gas flow. The evaporator temperatures for the precursors were as follows: 180 °C (**1**), 190 °C (**2**), 200 °C (**3**). Substrate temperatures: 600-750 °C. Carrier gas: argon. Reagent gas: oxygen. Flow rates: 30 mL/min and 100 mL/min, respectively. Total pressure: 20 Torr. Precursor weight: ~300 mg. The Si(100) 10×10 mm substrates were used for preliminary experiments. The deposition time was 60 min.

DLI MOCVD experiments

The experiments were carried out in a hot-wall quartz reactor equipped with an evaporator with a Kemstream injector [18]. 0.01 M solution (60 mL) of precursor **3** in heptane was used. Injection frequency: 2 Hz. Evaporator temperature: 180 °C. Substrate temperatures: 700 °C and 750 °C. Deposition time: 100 min. Carrier gas: nitrogen (400 mL/min). Reagent gas: oxygen (100 mL/min). Operating pressure: 3 Torr.

X-ray powder diffraction. The diffraction patterns of the films on silicon substrates were obtained on a Shimadzu XRD-7000 diffractometer (CuK_α radiation, Ni filter, 2 θ -scanning mode, θ range 5-65°, scanning step 0.03°, accumulation time 5 s, room temperature) and on a BRUKER RX D8 GIXRD diffractometer (grazing incidence X-Ray diffraction, CuK_α radiation, Ni filter, ω -2 θ - scanning, $\omega = 1^\circ$, step 0.02°, accumulation time 2 s). The diffraction patterns were indexed according to PDF (Powder Diffraction File, release 2010, International Centre for Diffraction Data, Pennsylvania, USA, <http://www.icdd.com/products/pdf2.htm>) and COD (Crystallography Open Database, <http://www.crystallography.net/cod>).

TABLE 1. Main Peaks of Ions in the Mass Spectra of Studied Precursors and Initial Homometallic Complexes

<i>m/z</i>	Ion peak assignments	Relative intensity (%) of compound ion peaks / evaporator temperature (°C)						
		1/208	2/216	3/229	Pb(hfa) ₂ /100	ZrL ₂ /220	PbL ₂ /150	La(dpm) ₃ /230
837	[ZrL ₃ (hfa)-C ₄ H ₉] ⁺	14	–	–	–	–	–	–
829	[ZrL ₄ -C ₄ H ₉] ⁺	16	–	–	–	–	–	–
805		–	22	–	–	–	–	–
742		–	16	–	–	–	–	–
704	[ZrPbL(hfa)] ⁺ /[ZrOHL ₃] ⁺	55	–	–	–	–	–	–
696	[ZrPbL ₂] ⁺ /[ZrL ₂ H(hfa)] ⁺	100	–	–	–	–	–	–
688	[La(dpm) ₃] ⁺	–	–	17	–	–	–	12
687	[ZrL ₃] ⁺	–	44	–	–	100	–	–
671	[ZrL ₂ (dpm) ₂] ⁺	–	–	50	–	–	–	–
655	[ZrL(dpm) ₂] ⁺	–	–	100	–	–	–	–
639	[Zr(dpm) ₃] ⁺	–	–	80	–	–	–	–
631	[La(dpm) ₃ -C ₄ H ₉] ⁺	–	–	–	–	–	–	40
622	[Pb(hfa) ₂] ⁺	–	–	–	11	–	–	–
557	[PbL(hfa)-C ₄ H ₉] ⁺	38	–	–	–	–	–	–
549	[PbL ₂ -C ₄ H ₉] ⁺	–	–	–	–	–	10	–
539		22	–	–	–	–	–	–
533	[PbL ₂ -C ₄ H ₉ O] ⁺	–	34	–	–	–	24	–
526		20	–	–	–	–	–	–
505	[ZrOHL ₂] ⁺	–	–	–	–	27	–	–
504	[La(dpm) ₂] ⁺	–	–	–	–	–	–	100
496	[ZrL(hfa)] ⁺	24	–	–	–	–	–	–
415	[ZrL ₂ -C ₄ H ₉ O] ⁺	79	–	–	–	–	–	–
	[Pb(hfa)] ⁺	–	–	–	100	–	–	–
407	[PbL] ⁺	–	100	–	–	–	100	–
403	[ZrL ₂ -COC ₄ H ₉] ⁺	52	–	–	–	–	–	–
389		–	49	–	–	–	–	–
376		19	66	–	–	–	62	–
366		21	–	–	–	–	–	–
346	[Pb(hfa)-CF ₂] ⁺	–	–	–	43	–	–	–
315		–	47	–	–	–	–	–
306	[ZrOHL] ⁺	18	–	–	–	23	–	–
239	[PbOCH ₃] ⁺	22	31	–	–	–	40	–
227	[PbF] ⁺	30	–	–	79	–	–	–
208	[Pb] ⁺	52	34	–	74	–	40	–

The coherent scattering region (CSR) was estimated by the Scherrer equation [19]. The diffraction line half-widths were calculated taking into account the hardware peak broadening with respect to the external silicon reference. The ZrO₂ cubic cell parameters were calculated using full-profile refinement with the PowderCell 2.4 program [20]. A Si (100) substrate was used as the internal reference.

Film morphology was examined by scanning electron microscopy (SEM) on a JEOL JSM6700F, microscope equipped with a JEOL EX-23000 BU energy dispersive X-ray (EDX) spectroscope.

X-ray photoelectron spectra (XPS) were recorded using a AlK_α monochromatic source ($h\nu = 1486.6$ eV) in the ThermoScientific K-Alpha system. The size of the studied area was ~ 400 μm. The analyzer energy was 30 eV (with a step of 0.1 eV) for core levels and 150 eV for survey spectra (with a step of 1 eV). The spectrometer was calibrated for Au4f_{7/2}

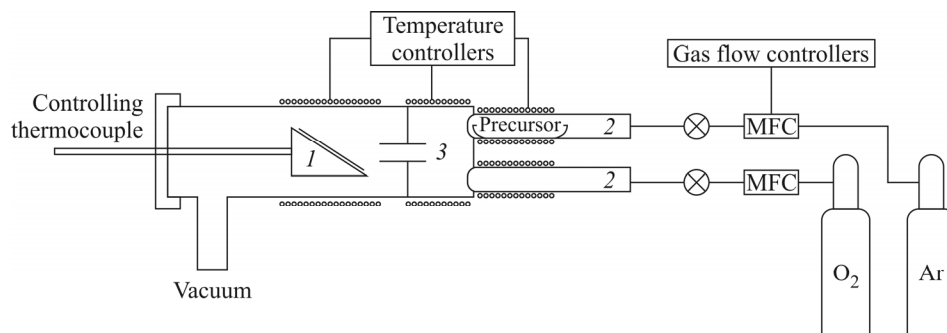


Fig. 2. Schematic hot-wall quartz reactor: susceptor (1), evaporator (2), mixer (3).

(83.9 ± 0.1 eV) and $\text{Cu}2p_{3/2}$ (932.8 ± 0.1 eV) lines. The XPS spectra were recorded in the direct mode using background subtraction with the Shirley method. The surface charge effect was eliminated using a slow electron source. The surface etching was performed with a 500 eV source of Ar^+ ions. The results were interpreted by using the data of the NIST XPS Database [21].

RESULTS AND DISCUSSION

Thermal properties of precursors

All obtained precursors were white fine-crystalline stable-in-air substances. To estimate the applicability of obtained compounds as MOCVD precursors, the main focus concerned the characterization of thermal properties. It was visually observed that the samples started melting when heated to $T > 200$ °C (Kofler bench). According to TGA data, the main weight loss occurs after the melting at $T > 200$ °C (Fig. 3). A one-stage weight loss process was observed only for **3**, while the amount of non-volatile residue (<5%) was comparable to that in **1** and **2**. The amount of the solid residue suggests that the weight loss process is more related to evaporation rather than to decomposition. Complete decomposition would yield ~28% of the residue. **1** is the most volatile fluorinated precursor. The proportion of the non-volatile residue for **2** and **3** is ~3%.

The composition of the gas phase obtained by heating the precursors at the evaporator temperature of 208 °C, 216 °C, 240 °C for precursors **1**, **2**, **3** was studied by mass spectrometry. The precursors at the above temperatures were in a molten state. The mass spectra of all studied precursors were not simple superpositions of the spectra of initial complexes (see the Table 1). Besides, heteroligand precursors **1** and **3** demonstrated ion peaks corresponding to the products of ligand exchange between homometallic components. The ligand exchange took place upon precursor heating. Thus, evaporation of **1**

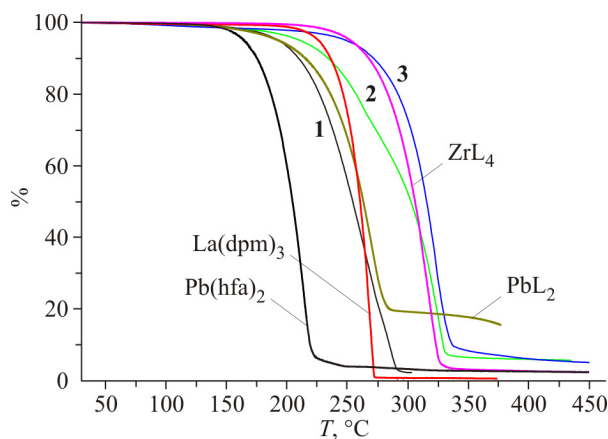


Fig. 3. TG curves of studied precursors compared with those of initial homometallic complexes.

and **3** leads to the incongruent evaporation of precursors. This thermal behavior seems to be typical of low-volatile compounds transforming into the gas phase from the melt, e.g. titanyl dipivaloylmethanate $\text{TiO}(\text{dpm})_2$ [22]. The precursor vapors injected into the MOCVD low-pressure hot-wall microreactor was further heated in the presence of oxygen to investigate their thermal stability and the composition of gaseous thermolysis products. The precursor **3** vapors were the most stable ones: the decomposition started at $T > 320$ °C for **3** and only at 270 °C and 280 °C for **1** and **2**, respectively. Fig. 4 shows temperature dependences mass spectrum peaks characterizing the gas phase composition upon heating the La–Zr precursor vapors. As can be seen, the changes in the peaks of metal-containing ions are sybatic, which means that they come from the same source. The main gaseous thermolysis product is a protonated ligand represented by the fragmented $[\textit{t}\text{-BuCOCHCO}]^+$ ion. We can say that the precursor thermolysis leading to the formation of oxides proceeds as a result of an intramolecular mechanism similar to that reported for $\text{Pb}(\text{dpm})_2$ in our earlier work [23]. Carbon oxides and water are products of deep oxidation of the precursor's organic part at high temperatures. Note that the mass spectrum was generally reproduced for all precursors after cooling the reactor, though the intensity of its peaks decreased. This means that the precursor shows satisfactory stability under isothermal evaporation in the course of the experiment (1.5 h). However, the stability decreases with time: long-term heating causes thermal transformations associated with the accumulation of non-volatile products while the mass spectrum peak intensities are decreased. Obviously, not only the composition and structure of the deposited film but also the reproducibility of these properties will be affected by such thermal behavior of precursors. Reducing the evaporation temperature is one possible way to overcome this problem.

Film preparation and examination

Since the thermal behavior of low-volatile precursors showed that evaporation in vacuum is far from being the best option, a carrier gas was used to reduce evaporation temperatures without lowering the precursor concentration in the deposition zone. The films were prepared for deposition temperatures of 600-750 °C. According to reported data, ZrO_2 -based films prepared at 600 °C and 650 °C are too thin and poorly crystallized. A similar situation was observed for precursors **1-3**. Therefore, the films (white-grayish coatings) considered below were synthesized at 700 °C and 750 °C. The Scotch tape test showed good adhesion to substrates. Fig. 5 juxtaposes GIXRD data for the films prepared from **1**. The main crystalline phase of the films is a solid solution based on ZrO_2 tetragonal and cubic modifications. Tetragonal ZrO_2 is very common in

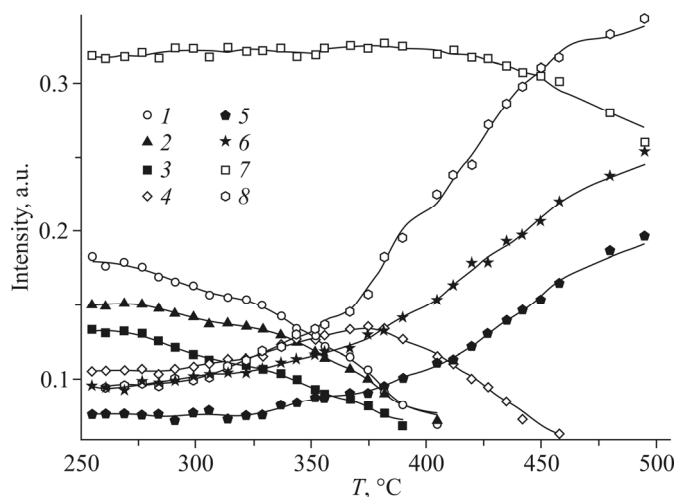


Fig. 4. Temperature dependences of mass spectrum ion peak intensities characterizing the gas phase composition upon heating the vapors of **3**: $[\text{ZrL}_2(\text{dpm})_2]^+$ (**1**); $[\text{ZrL}(\text{dpm})_2]^+$ (**2**); $[\text{Zr}(\text{dpm})_3]^+$ (**3**); $[\textit{t}\text{-BuCOCHCO}]^+$ (**4**); $[\text{H}_2\text{O}]^+$ (**5**); $[\text{CO}]^+$ (**6**); $[\text{O}_2]^+$ (**7**); $[\text{CO}_2]^+$ (**8**).

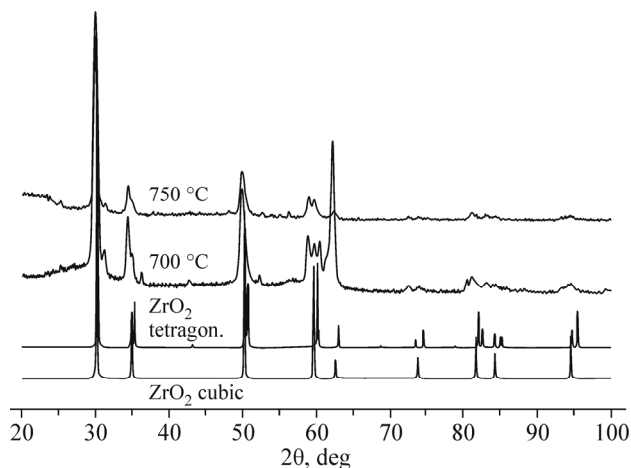


Fig. 5. Comparison of GIXRD data for the films prepared from **1** at 700 °C and 750 °C.

MOCVD films, even though it is metastable at such temperatures. The stabilization of this phase is usually explained by fine crystallinity and low film thickness resulting in such deposition conditions that the nucleation rate exceeds the rate of surface diffusion [24]. According to EDS data, the Pb/Zr atomic ratio in the films is ~ 1:25 (650 °C), 1:7 (700 °C), 1:4 (750 °C). The significant enrichment of the films by the Zr component can be explained by the fact that the precursor dissociates into monometallic complexes near the heated substrate whereby the most volatile component $\text{Pb}(\text{hfa})_2$ is mainly eliminated without being decomposed. As the temperature rises, more of this component has time to decompose on the substrate, and the lead content increases. Lead is not the main component of the film and, according to the XRD data, it does not form separate phases. Therefore, a question arises as to what form it adopts inside the films. To find it out, the XPS data were analyzed. Fig. 6 compares $\text{Pb}4f_{7/2}$ lead lines before and after etching the film surface. After etching, the bands shift to higher energies for all components ($\text{O}1s$, $\text{F}1s$, $\text{C}1s$, $\text{Si}2p$, $\text{Zr}3d$, $\text{Pb}4f$), possibly due to the fact that some charge appeared on the sample surface. Before etching, lead on the sample surface can occur in $\text{Pb}(\text{OH})_2$ (138.2 eV) or PbCO_3 (138.3 eV) forms. After etching, there is a weak signal at ~136.6 eV (corrected) which is clearly seen against the background of the main lead line and can be assigned to Pb^0 . By now, it is hard to tell if metallic lead is a film component or appears as a result of Ar^+ etching, even though we reported previously that MOCVD metal-lead films can be obtained from fluorinated lead diketonates at 450-

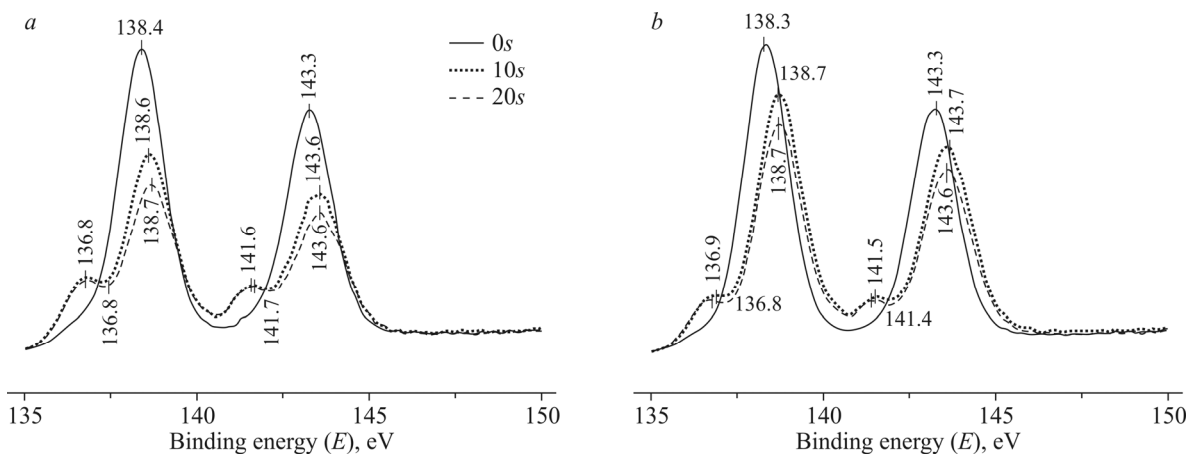


Fig. 6. Comparison of $\text{Pb}4f_{7/2}$ photoelectron lines for the films prepared from **1** at 700 °C (a) and 750 °C (b) before and after etching.

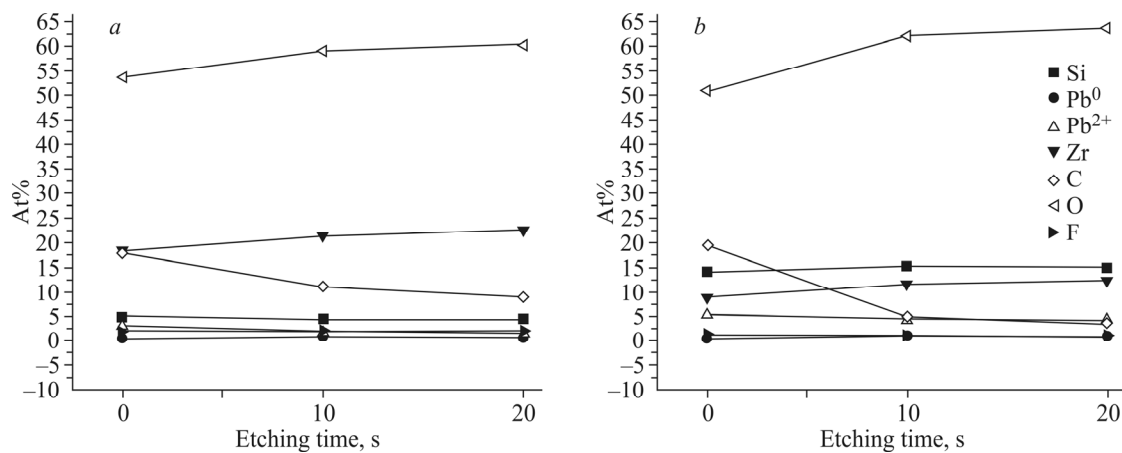


Fig. 7. Comparison of elemental compositions (according to XPS) of the films prepared from **1** at 700 °C (a) and 750 °C (b) before and after etching.

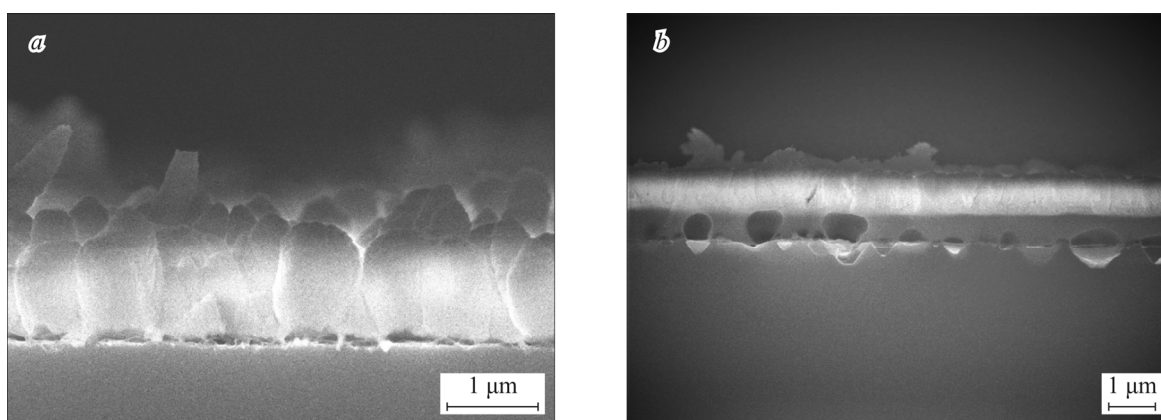


Fig. 8. SEM images of transverse fractures of the prepared from **1** at 700 °C (a) and 750 °C (b), respectively.

500 °C [23, 25]. Fig. 7 juxtaposes atomic concentrations of components in the course of film etching, according to XPS data. As can be seen, the fluorine content is too low to conclude that all lead is bound in PbF₂ (138.5-139.1 eV). Besides, carbon content decreases within the bulk of the film, while silicon content increases, especially at 750 °C. This agrees with the SEM data (Fig. 8) indicating the formation of an intermediate layer due to interdiffusion of film and substrate materials. Therefore, we believe that lead in the Pb⁺² form is simply dissolved within the ZrO₂ matrix. For comparison, the Pb4f_{7/2} line in PbZrO₃ occurs at 138.5 eV.

Fig. 8 shows the microstructure of cross sections of the films prepared from **1**. The films consist of ~0.5×1 μm vertical aggregates. At 750 °C, a thick intermediate layer is formed due to the reciprocal diffusion of film and substrate materials. Since powder XRD showed no silicate or silicide crystalline phases, we assume that this layer is amorphous. The caverns were formed as a result of material separation upon sample fracturing rather than on the sites of cavities in the film or in the substrate. At 700 °C, no such interface is formed for the same film thickness. Obviously, a further increase of the deposition temperature is undesirable for the preparation of ZrO₂-based films on silicon substrates.

In the same conditions, non-fluorinated precursor **2** was used to prepare films with the Pb/Zr metal ratio of ~ 1:1 (700 °C) and 5:4 (750 °C), as is indicated by EDX. Thus, in the case of the homoligand non-fluorinated precursor, the metal ratio in the film repeats that of the precursor. The main crystalline phases of the films are tetragonal [JCPDS 010-070-7360] and cubic [JCPDS 000-49-1642] modifications of the ZrO₂ solid solution (Fig. 9). Only the second modification can be stabilized by lead impurities. The diffraction patterns of the films exhibit broad peaks, possibly due to small thickness and fine-crystalline structure of the film. Further, the size of ZrO₂ crystallites was estimated. The CSR calculated with respect to

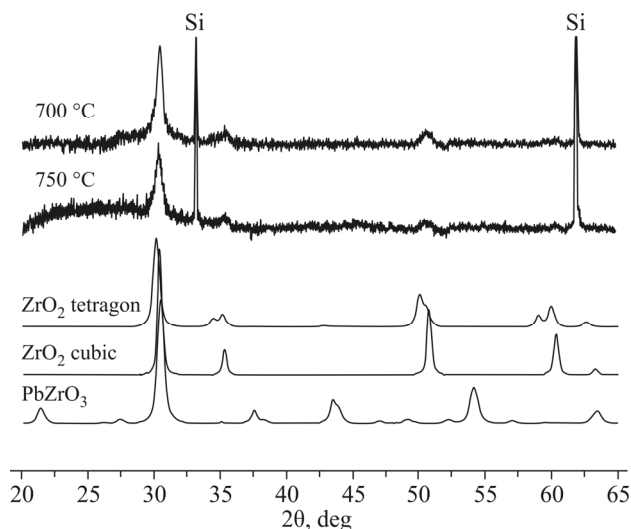


Fig. 9. Comparison of XRD data for the films prepared from **2** at 700 °C and 750 °C.

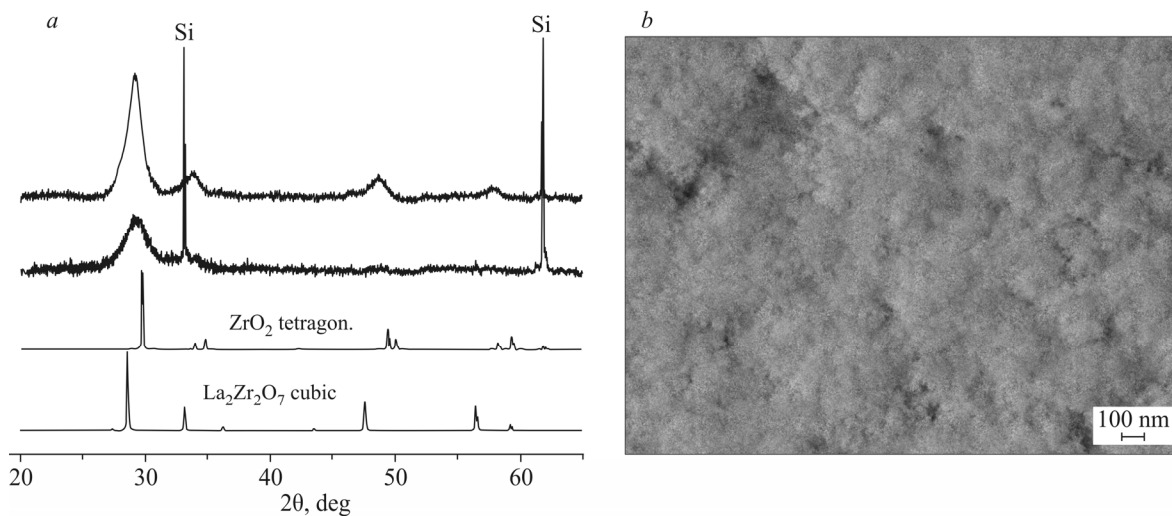


Fig. 10. Comparison of XRD data (*a*) and SEM images of surfaces (*b*) for the films prepared from **3** at 700 °C and 750 °C, respectively.

peak (111) was ~ 16 nm. As the deposition temperature increased from 700 °C to 750 °C, the CSR size did not change. The parameters of ZrO_2 cubic cell are 5.127(3) Å and 5.129(3) Å for the films prepared at 700 °C and 750 °C, respectively. Within the measurement accuracy, these values coincide with the cell parameter of pure ZrO_2 [JCPDS 000-49-1642] (5.128 Å). A more accurate calculation is hindered by the presence of the ZrO_2 tetragonal phase and by low peak intensities in the region of large angles. Since the obtained films are fairly thin (~ 200 nm), further research with this precursor are required to optimize the deposition process.

According to powder XRD, non-stoichiometric nanocrystalline $\text{La}_2\text{Zr}_2\text{O}_7$ seems to be the main phase of the films prepared from **3** (Fig. 10*a*). As can be seen from the SEM image, the film looks “like snow”, i.e. it is too finely crystalline (Fig. 10*b*).

Estimating the size of $\text{La}_2\text{Zr}_2\text{O}_7$ crystallites

The CSR calculated with respect to peak (222) is ~ 7 nm at 700 °C. At 750 °C, the crystallite size decreases to 5 nm. The zirconium-lanthanum precursor showed the most interesting results in terms of obtaining a mixed-oxide phase. Therefore, we studied DLI MOCVD films using a solution of this precursor. This method is well adapted for low-volatile

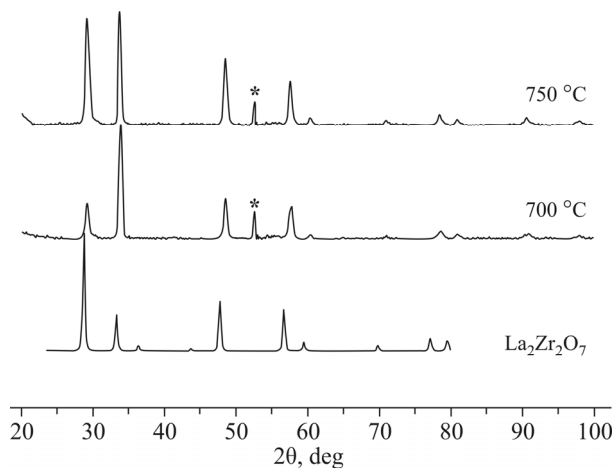


Fig. 11. Comparison of GIXRD data for the films prepared from **3** by DLI CVD at 700 °C and 750 °C, respectively; * is the substrate signal.

precursors. Lanthanum zirconate films were prepared on silicon and stainless steel substrates. The GIXRD data for the samples synthesized at 750 °C and 700 °C correspond to $\text{La}_2\text{Zr}_2\text{O}_7$ JCPDS [01-074-9307], all peaks being shifted (Fig. 11). The obtained results suggest that homometallic fragments of precursor **3** in the non-coordinating solvent solution remain bound, thereby providing the stoichiometry of the films.

CONCLUSIONS

The composition and structure of multicomponent ZrO_2 -based films prepared by metalorganic chemical vapor deposition using mixed bimetal precursors containing methoxy-substituted β -diketonates are determined by the precursor composition. Thermal properties of a precursor are significantly affected by its composition. The zirconium-lead precursor **1** demonstrates high volatility due to the presence of fluorine-containing substituents in the ligand. However, in contrast to previously studied copper-palladium precursors, this fact does not enhance the precursor's thermal stability with respect to the dissociation into monometallic complexes; instead, the assumed stoichiometry of the film is changed due to the removal of a more volatile component, a homometallic complex, from the deposition zone. Among mixed zirconium-containing precursors, most promising are the systems whose ligands do not contain fluorine. The example of the zirconium-lanthanum precursor **3** proves the possibility of using metalorganic chemical vapor deposition for the preparation of $\text{La}_2\text{Zr}_2\text{O}_7$ -containing films with two modes of the precursor vapor supply: 1) evaporation in the carrier gas flow and 2) direct liquid injection. In the case of low-volatile precursors, thermal transformations in the condensed phase is to be prevented to avoid the formation of films with uncontrolled composition. This can be achieved by decreasing the evaporation temperature, e.g., by using the DLI system of precursor supply.

FUNDING

The reported study was funded by RFBR and CNRS (projects 18-53-15005 and PRC 1986/2018, respectively).

CONFLICT OF INTERESTS

The authors declare that they have no conflict of interests.

REFERENCES

1. R. Vassen, M. O. Jarligo, T. Steinke, D. E. Mack, and D. Stöver. *Surf. Coat. Technol.*, **2010**, 205(4), 938.
2. C. Haering, A. Roosen, H. Schichl, and M. Schnöller. *Solid State Ionics*, **2005**, 176(3–4), 261.
3. E. J. Harvey, K. R. Whittle, G. R. Lumpkin, R. I. Smith, and S. A. T. Redfern. *J. Solid State Chem.*, **2005**, 178(3), 800.
4. G. Yang, D. Wang, C. Zhang, J. Cao, Y. Du, B. Liu, H. Chen, Y. Cui, H. Luo, and Y. Gao. *Ceram. Int.*, **2019**, 45, 4926.
5. N. Izyumskaya, Y.-I. Alivov, S.-J. Cho, H. Morkoç, H. Lee, and Y.-S. Kang. *Crit. Rev. Solid State Mater. Sci.*, **2007**, 32(3–4), 111.
6. A. Devi. *Coord. Chem. Rev.*, **2013**, 257, 3332.
7. L. G. Hubert-Pfalzgraf. *Inorg. Chem. Commun.*, **2003**, 6, 102.
8. M. Veith, *J. Chem. Soc., Dalton Trans.*, **2002**, 2405.
9. V. V. Krisyuk, Y. V. Shubin, F. Senocq, A. E. Turgambaeva, T. Duguet, I. K. Igumenov, and C. Vahlas. *J. Cryst. Growth*, **2015**, 414, 130.
10. V. V. Krisyuk, S. Urkasym kyzy, I. A. Baidina, G. V. Romanenko, I. V. Korolkov, T. P. Koretskaya, N. I. Petrova, and A. E. Turgambaeva. *J. Struct. Chem.*, **2017**, 58(8), 1522.
11. M. Veith, M. Bender, T. Lehnert, M. Zimmer, and A. Jakob. *Dalton Trans.*, **2011**, 40, 1175.
12. J. H. Thurston, D. Trahan, T. Ould-Ely, and K. Whitmire. *Inorg. Chem.*, **2004**, 43, 3299.
13. N. Kuzmina, I. Malkerova, M. Ryazanov, A. Alikhanyan, A. Rogachev, and A. N. Gleizes. *J. Phys. IV*, **2001**, 11, Pr3-661.
14. V. V. Krisyuk, I. A. Baidina, and I. K. Igumenov. *Main Group Met. Chem.*, **1998**, 21(4), 199.
15. A. E. Turgambaeva, V. V. Krisyuk, I. A. Baidina, I. V. Korolkov, I. Yu. Ilyin, S. Urkasym kyzy, and I. K. Igumenov. *J. Struct. Chem.*, **2017**, 58(8), 1530.
16. L. Yuikhan, S. A. Mosyagina, P. A. Stabnikov, N. I. Alferova, I. V. Korol'kov, N. V. Pervukhina, and N. B. Morozova. *J. Struct. Chem.*, **2017**, 58(4), 843.
17. A. Turgambaeva, N. Prud'homme, V. Krisyuk, and C. Vahlas. *Chem. Vap. Deposition*, **2012**, 18, 209.
18. L. Baggetto, J. Esvan, C. Charvillat, D. Samélor, H. Vergnes, B. Caussat, A. Gleizes, and C. Vahlas. *Phys. Status Solidi C*, **2015**, 12(7) 989.
19. V. I. Iveronova and G. P. Revkevich. *Teoriya Rasseyaniya Rentgenovskikh Luchey (X-Ray Scattering Theory)* [in Russian]. Mos. Gos. Univ.: Moscow, **1978**.
20. W. Kraus and G. Nolze. *J. Appl. Crystallogr.*, **1996**, 29, 301.
21. A. V. Naumkin, A. Kraut-Vass, S. W. Gaarenstroom, and C. J. Powell. NIST Standard Reference Database 20, Version 4.1. **2012**. <http://srdata.nist.gov/xps/>.
22. A. E. Turgambaeva and I. K. Igumenov. *J. Phys. IV*, **2001**, 11, Pr3-621.
23. V. V. Krisyuk, A. E. Turgambaeva, and I. K. Igumenov. *Chem. Vap. Deposition*, **1998**, 4(2), 43.
24. Z. Chen, N. Prud'homme, B. Wang, P. Ribot, and V. Ji. *Surf. Coat. Technol.*, **2013**, 218, 7.
25. A. E. Turgambaeva, A. F. Bykov, V. V. Krisyuk, and I. K. Igumenov. *Thermochim. Acta*, **1997**, 307, 85.